

Conductance as a Function of the Temperature in the Double Exchange Model

M.J. Calderón^{1,2}, J.A.Vergés¹ and L. Brey¹

¹*Instituto de Ciencia de Materiales de Madrid, Consejo Superior de Investigaciones Científicas.
28049 Cantoblanco, Madrid, Spain.*

²*Departamento de Física Teórica de la Materia Condensada, Facultad de Ciencias, Universidad Autónoma de Madrid, 28049 Cantoblanco, Madrid, Spain.
(January 6, 2018)*

We have used the Kubo formula to calculate the temperature dependence of the electrical conductance of the double exchange Hamiltonian. We average the conductance over an statistical ensemble of clusters, which are obtained by performing Monte Carlo simulations on the classical spin orientation of the double exchange Hamiltonian. We find that for electron concentrations bigger than 0.1, the system is metallic at all temperatures. In particular it is not observed any change in the temperature dependence of the resistivity near the magnetical critical temperature. The calculated resistivity near T_c is around ten times smaller than the experimental value. We conclude that the double exchange model is not able to explain the metal to insulator transition which experimentally occurs at temperatures near the magnetic critical temperature.

PACS number 71.10.-w, 75.10.-b

I. INTRODUCTION

Materials that present extremely large magnetoresistance have potential technological applications. As mixed valence compounds of the form $La_{1-x}^{3+}A_x^{2+}Mn_{1-x}^{3+}Mn_x^{4+}O_3^{2-}$ (where A can be Ca, Sr or Ba) show colossal magnetoresistance there is a renewed interest in these oxides with perovskite structure [1,2]. There is a big correlation between the magnetic and the transport properties of these oxide manganites. For $0.1 \leq x \leq 0.5$ and low temperatures, the system is metallic and presents ferromagnetic order. As the temperature (T) increases the system becomes insulator and paramagnetic. The metallic (insulator) behavior is defined in the sense that $d\rho/dT > 0$ ($d\rho/dT < 0$), being ρ the electrical resistivity. In the insulating phase the resistivity is bigger than the Mott resistivity $\sim 1000\mu\Omega - cm$ [3]. The magnetic transition occurs at a x -dependent critical temperature $T_c \sim 300K$. The metal to insulator transition occurs at a temperature very close to T_c . For $x \rightarrow 0$ and low temperatures the system is a layer antiferromagnet with ferromagnetic coupling inside planes. At $x \leq 0.1$ phase separation between hole-rich and hole-poor regions has been predicted [4–6]. The electron-electron interaction plays an important role at low temperatures, and it produces charge ordering at particular values of $x < 0.5$ and always for values of $x \geq 0.5$ [7].

In the Mn oxides the electronically active orbitals are believed to be the $Mn d$ orbitals, and the mean d occu-

pancy is $4 - x$. The Mn ions are located at the corners of a simple cubic lattice, and they feel the cubic crystal symmetry, which splits the d orbitals into a t_{2g} triplet and a e_g doublet. There is also a strong ferromagnetic Hund's rule coupling which align all electron spins in the $Mn d$ orbitals. The physical picture is that three electrons fill up the t_{2g} levels forming a core spin S of magnitude $3/2$ and the rest of the electrons go to the e_g orbitals. For small values of x , the perovskites show a long-range Jahn-Teller order which selects a preferred combination of the e_g orbitals and therefore it is possible to assume that the electrons move only through one d orbital.

To explain the ferromagnetism in these materials Zener [8] introduced a double exchange (DE) mechanism, in which the electrons get mobility between the Mn ions using the magnetically inert oxygen as an intermediate. The oxygens are located at the center of the lines connecting the Mn ions. This conduction process is proportional to the electron transfer integral and due to the strong ferromagnetic Hund's rule coupling it is maximum when the two cores spins involved in the process are parallel and it is zero when they are antiparallel. So in the DE model ferromagnetic coupling between Mn^{3+} and Mn^{4+} arises from the hopping of the electrons in the e_g orbitals. Because the alignment of spins on neighboring sites favors electronic motion, the ferromagnetic ground state maximize the electron kinetic energy. When the temperature increases, the DE model undergoes a phase transition towards a paramagnetic state. In this phase the core spins are randomly oriented and fluctuate at frequencies related only to the temperature. In the paramagnetic phase the electrons minimize their kinetic energy. The DE model was more precisely formulated and extended by Anderson and Hasegawa [9] and by de Gennes [10].

Mean field theories have shown that the ferro to paramagnetic phase transitions at T_c is accompanied by a change in the temperature dependence of the resistivity [11–14]. However these calculations do not show metal to insulator transition at temperatures near T_c . These mean field calculations do not take into account the effect of the Berry phase arising from particle motion in a spin background [15]. Also the possible localization of electrons by the spin disorder in the paramagnetic phase is neglected. Varma [16] proposed that random hopping in the paramagnetic phase is sufficient to localize electrons and induce a metal to insulator transition at the

magnetic critical temperature. However Li *et al* [17] have studied the mobility edge of the DE model in the limit of $T \rightarrow \infty$ and they have found that random hopping alone is not enough to induce Anderson localization at the Fermi level in the range $0.1 \leq x \leq 0.4$. Similar results were reported by Allub and Alascio [18] using the Ziman criterion [19].

In this work we study the temperature dependence of the electric conductance of the DE model for different values of the electron concentration. We find that the system is metallic at all temperatures and, contrary to the mean field results, we do not observe any feature in the temperature dependence of the resistivity near the magnetic critical temperature.

We calculate the dc conductance, G , by using the Kubo formula. We perform Monte Carlo simulations on the classical spin orientations of the DE model [20], and for each electron concentration and temperature we obtain a statistical ensemble of clusters of Mn ions. We obtain the conductance by averaging over several configurations. The temperatures we are interested are $T \leq 500K$ ($T_c \sim 300K$) and these temperatures are much smaller than the electron Fermi temperature for $x \geq 0.1$. Therefore we always consider, both in the Monte Carlo simulations and in the conductance calculations, that the electron temperature is zero.

In our model the Mn ion spins are treated as classical and quantum effects, as absorption and emission of spin density waves, are not correctly described. Although quantum effects should be important at very low temperatures [11], they do not matter at temperatures near T_c .

The paper is organized as follows, in section II we introduce the DE Hamiltonian and describe the Monte Carlo calculations. In section III we give some remarks about the use of the Kubo formula in the present context. Section IV is dedicated to present and discuss the results of the paper, and we finish in section V with a summary.

II. DOUBLE EXCHANGE HAMILTONIAN.

For large Jahn-Teller splittings, the electronic and magnetic properties of the Mn oxides are described by the following ferromagnetic Kondo lattice Hamiltonian [9],

$$\hat{H} = -t \sum_{\langle i,j \rangle, \sigma} \left(\hat{C}_{i,\sigma}^+ \hat{C}_{j,\sigma} + h.c. \right) - J_H \sum_{i,\sigma,\sigma'} \hat{C}_{i,\sigma}^+ \sigma_{\sigma,\sigma'} \hat{C}_{i,\sigma'} \cdot \mathbf{S}_i, \quad (1)$$

where $\hat{C}_{i,\sigma}^+$ creates an electron at site i and spin σ , \mathbf{S}_i represents the classical core spin at site i , t is the hopping amplitude between nearest-neighbor sites and J_H is the Hund's rule coupling energy. In the limit of infinite J_H , Eq.(1) becomes the DE Hamiltonian,

$$\hat{H}_{DE} = - \sum_{\langle i,j \rangle} \left(t_{i,j} \hat{C}_i^+ \hat{C}_j + h.c. \right), \quad (2)$$

Here \hat{C}_i^+ creates an electron at site i with spin parallel to \mathbf{S}_i , and the hopping amplitude acquires a Berry phase and it becomes a complex number given by [15],

$$t_{i,j} = t \left(\cos \frac{\theta_i}{2} \cos \frac{\theta_j}{2} + \sin \frac{\theta_i}{2} \sin \frac{\theta_j}{2} e^{i(\phi_i - \phi_j)} \right), \quad (3)$$

where θ_i and ϕ_i are the angles which characterize the orientation of \mathbf{S}_i . This complex hopping appears after rotating the conduction electron spins so that the spin quantization axis at site i is parallel to \mathbf{S}_i , and then project onto the spin parallel to \mathbf{S}_j .

In order to calculate the electrical conductance, for each T and x , it is necessary a statistical ensemble of clusters, which simulates the thermal fluctuations. Each cluster is characterized by a set of core spin $\{\mathbf{S}_i\}$ and its chemical potential μ . We obtain the clusters by performing Monte Carlo simulations on the variables θ_i and ϕ_i of the Hamiltonian Eq.(2). In each Monte Carlo step it is necessary to diagonalize a matrix of size equal to the number of Mn ions in the clusters and the DE energy is the sum of the eigenenergies of the occupied electron levels. In this process we assume that the electron Fermi energy is much bigger than the temperatures of interest in this work (at $x \sim 0.2$, $T_{Fermi} \sim 2000K$ and $T_c \sim 300K$). The diagonalization imposes a restriction on the dimension of the unit cell used in the simulations. Recently two of us have studied, by using Monte Carlo simulations, the magnetic phase diagram of the DE model [20]. To avoid finite size problems in the simulation, the following approximation for the energy has been obtained and used for the DE energy,

$$E \simeq -2t \langle \hat{C}_i^+ \hat{C}_j \rangle_0 \sum_{\langle i,j \rangle} \cos \frac{\theta_{ij}}{2} - a_2 \sum_{\langle i,j \rangle} (\bar{t} - t_{i,j})^2. \quad (4)$$

Here $\langle \hat{C}_i^+ \hat{C}_j \rangle_0$ and a_2 are quantities which depend on x and do not depend on temperature, \bar{t} is the average of the absolute value of the hopping amplitude and $\theta_{i,j}$ represents the angle formed by the core spins located at sites i and j . In reference [20] it was showed that expression (4) is a good approximation to the DE kinetic energy. In that work it was also concluded that the magnetic critical temperatures of the DE model are in the range of the experimental ones, and it was obtained that the complex phase of the hopping amplitude has a negligible effect in the value of T_c .

Using the conclusions of the cited work, in this paper we perform Monte Carlo simulations on the variables θ_i and ϕ_i , using the expression (4) for the DE energy. The simulations are performed in $N \times N \times N$ cubic lattices. Technical details about the Monte Carlo calculations are given in reference [20], here just say that typically 5000-7000 Monte Carlo steps per spin are used for thermal

equilibration. The different clusters which form the statistical ensemble are chosen every 100 steps per spin after equilibration.

III. D.C. CONDUCTANCE VIA KUBO FORMULA

In calculating the conductance of the system we use the standard Kubo formula [21,22]. The static electrical conductivity at chemical potential μ is given by

$$G = \sigma_{zz}(0) = -2 \frac{e^2}{h} \text{Tr} \left[(\hbar \hat{v}_z) \text{Im} \hat{\mathcal{G}}(\mu) (\hbar \hat{v}_z) \text{Im} \hat{\mathcal{G}}(\mu) \right], \quad (5)$$

where $\text{Im} \hat{\mathcal{G}}(\mu)$ is calculated from the advanced and retarded Green functions

$$\text{Im} \hat{\mathcal{G}}(\mu) = \frac{1}{2i} \left[\hat{\mathcal{G}}^R(\mu) - \hat{\mathcal{G}}^A(\mu) \right],$$

and the velocity (current) operator \hat{v}_z is related to the position operator \hat{z} through the equation of motion

$$\hbar \hat{v}_z = \left[\hat{H}, \hat{z} \right], \quad (6)$$

\hat{H} being the Hamiltonian in Eq. (2).

Numerical calculations are carried out for a bar geometry connecting the $N \times N \times N$ cluster to two ideal semiinfinite leads of $N \times N$ cross section. This provides complex selfenergies at opposite sides of the sample [22]. They are first calculated for the normal modes of the lead and then transformed to the local tight-binding basis. Specifically, the retarded selfenergy due to the mode of wavevector (k_x, k_y) at energy ε is given by:

$$\Sigma(k_x, k_y) = \frac{1}{2t} \left(\varepsilon - \varepsilon(k_x, k_y) - i \sqrt{4t^2 - (\varepsilon - \varepsilon(k_x, k_y))^2} \right),$$

within its band and by:

$$\Sigma(k_x, k_y) = \frac{1}{2t} \left(\varepsilon - \varepsilon(k_x, k_y) \mp \sqrt{(\varepsilon - \varepsilon(k_x, k_y))^2 - 4t^2} \right),$$

outside the band (minus sign for $\varepsilon > \varepsilon(k_x, k_y)$ and plus sign for $\varepsilon < \varepsilon(k_x, k_y)$), where $\varepsilon(k_x, k_y) = 2t(\cos(k_x) + \cos(k_y))$ is the eigenenergy of the (k_x, k_y) mode). The transformation from normal modes to the local tight-binding basis is obtained from the amplitudes of the normal modes:

$$\langle (n_x, n_y) | (k_x, k_y) \rangle = \frac{2}{N+1} \sin(k_x n_x) \sin(k_y n_y),$$

where n_x and n_y represent the tight-binding orbital position. Once the selfenergy matrices introduced by the left (right) semiinfinite leads are determined, the retarded Green function matrix of the sample $\mathbf{G}(\varepsilon)$ is defined by the following set of $N \times N \times N$ linear equations:

$$[\varepsilon \mathbf{I} - \mathbf{H} - \Sigma_l(i\varepsilon) - \Sigma_r(\varepsilon)] \mathbf{G}(\varepsilon) = \mathbf{I}, \quad (7)$$

where $\Sigma_{l(r)}(E)$ stand for the selfenergy matrices introduced by the left (right) semiinfinite leads. This set of equations is efficiently solved using a layer by layer inversion scheme that takes advantage of the band structure of the coefficients matrix. The advanced Green function matrix is simply the conjugate of the transpose of the retarded one.

The last ingredient that is necessary for the evaluation of the Kubo formula is the velocity operator. It is obtained through Eq.(6) once the position operator \hat{z} is known. This operator is determined by the spatial shape of the electric potential energy. Taking advantage from the fact that the detailed form of the electric field does not matter within one-electron linear response theory, an abrupt potential drop at one of the two cluster sides provides the simplest numerical implementation of the Kubo formula [23]. Certainly, Eq.(6) shows that nonvanishing elements of the velocity operator are restricted to the two layers at the sides of the potential drop. Furthermore, the trace appearing in Eq.(5) makes the knowledge of the Green functions on the same restricted set of sites enough for the evaluation of the conductance. Consequently, Green functions are just evaluated for two consecutive layers at the cluster boundary.

IV. RESULTS

We start showing the results corresponding to a perfect ferromagnetic system. In Fig.1a we plot the conductance as a function of the chemical potential for a cluster of size $N=20$ at $T=0$. The conductance is finite for chemical potentials in the range $-6t \leq \mu \leq 6t$. This is the range of energies where the density of states of the perfect system is finite, see Fig.1b. Since at $T=0$ all core spins are aligned, the transport in the system is ballistic and the conductance is just limited by the size of the cluster. Therefore, at $T=0$ the conductance is proportional to the number of transport channels at the Fermi energy, which for large clusters increases as N^2 . We have verified this behavior for $N \geq 10$ and also we have checked that for system sizes bigger than $N=10$, the overall shape of G does not depend on the cluster size.

In the opposite limit we have calculated the conductance in the paramagnetic phase at $T \rightarrow \infty$. In this limit the orientation of the local spins $\{\mathbf{S}_i\}$ is random. We choose \mathbf{S}_i to be uniformly distributed on a sphere, i.e. the probability P of having a core spin with azimuthal angle ϕ_i is $1/2\pi$, whereas the polar angle distribution verifies $P(\cos \theta_i) = 1/2$.

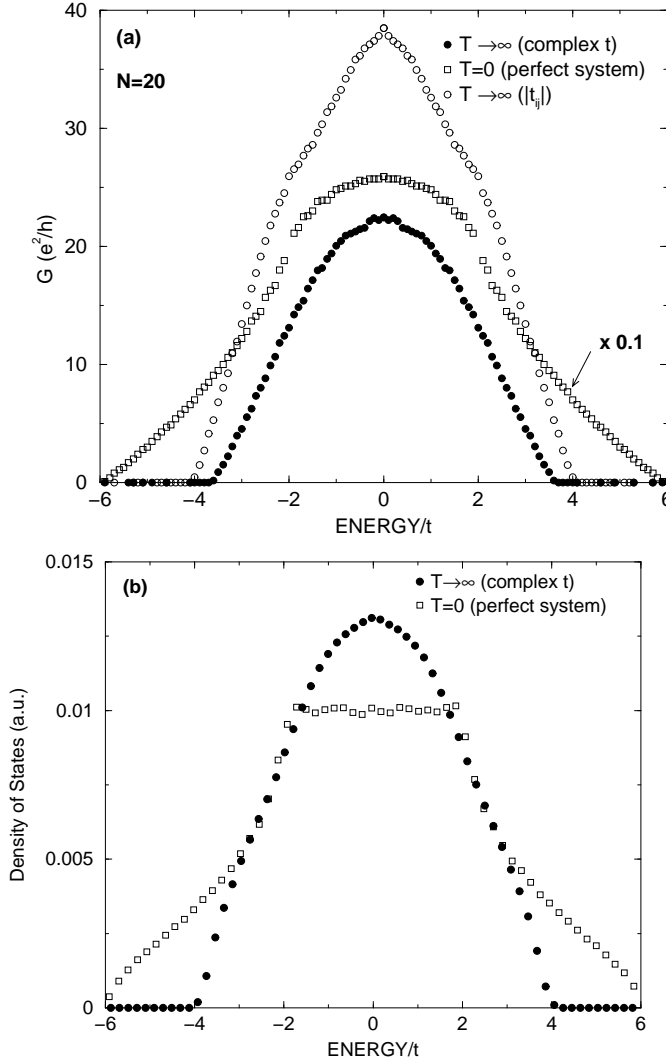


FIG. 1. a) Energy dependence of the conductance for the $T = 0$ case (empty squares), the $T \rightarrow \infty$ case (filled dots), and the $T \rightarrow \infty$ case without Berry's phase (empty dots). b) Density of states as a function of the energy for the $T = 0$ case (empty squares) and the $T \rightarrow \infty$ case (filled dots).

In Fig.1 we plot the conductance and the density of states as a function of the energy in the $T \rightarrow \infty$ limit. This quantities are averaged on many configurations of clusters of size $N=20$. The density of states shows an effective band edge at $E_b \simeq -4t$. This occurs because the average value of the absolute value of the hopping amplitude at $T \rightarrow \infty$ is $\langle |t_{i,j}| \rangle = 2/3 t$. Although the band edge starts at $-4t$, G is different from zero only for values of the chemical potential in the range $-3.6t \leq \mu \leq 3.6t$. The difference between the band edge energy and the minimum energy with $G \neq 0$ is due to the fact that all the states with energy $-4t < E < -3.6t$ are localized and do not contribute to G . Therefore $E_c \simeq -3.6t$ is the $T \rightarrow \infty$ mobility edge of the DE model. This result is in agreement with localization length calculations [17], which located the mobility edge at $|E_b| \simeq 3.56t$. Our

calculations show that $|E_b|$ is constant for values of N bigger than $N=10$. This implies that for energies lower than E_b the localization length is shorter than 10 lattice parameters. For $N \geq 10$, the overall shape of the average conductance as a function of energy is almost independent of the cluster size, and its value increases linearly with N . This implies that in the $T \rightarrow \infty$ limit the system is metallic, the electron transport is diffusive and the system verifies the Ohm's law: the cluster resistance is proportional to the cluster length and inversally proportional to the cross-sectional area. The proportionality constant is the resistivity ρ .

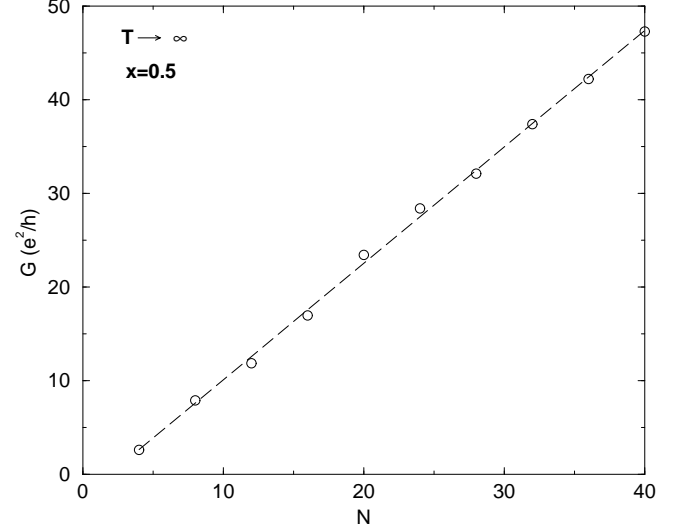


FIG. 2. Conductance as a function of the cluster size, for $x = 0.5$ and $T \rightarrow \infty$. The dashed line is only a guide to the eye.

As an example of this behavior we plot in Fig.2 the average conductance at $\mu = 0$ as a function of the cluster size N . The linear behavior of G versus N down to $N=4$, implies that the elastic mean free path is smaller than 4 lattice parameters. The slope of the straight line is the conductivity, in lattice parameter units, of the DE model at $T \rightarrow \infty$ and $x=0.5$.

In Fig.1 we also plot the average conductance in the $T \rightarrow \infty$ limit of the DE model but neglecting the Berry's phase in the hopping amplitude i.e. $t_{i,j} \rightarrow |t_{i,j}|$. In this case G is bigger than in the case of complex hopping. Also it seems that the mobility edge appears at lower energies than in the complex hopping DE model.

The previous calculations correspond to the $T=0$ and $T \rightarrow \infty$ limits. Now we present the results for G as a function of T , for different values of x . In these case the average of G is done with an statistical ensemble of clusters which are obtained from Monte Carlo calculations as described in Section II. When T increases the disorder in the system increases and two main effects occurs: a) a T -dependent mobility edge appears at low energies and b) the extended states acquire an elastic mean free path,

ℓ , which decreases with T .

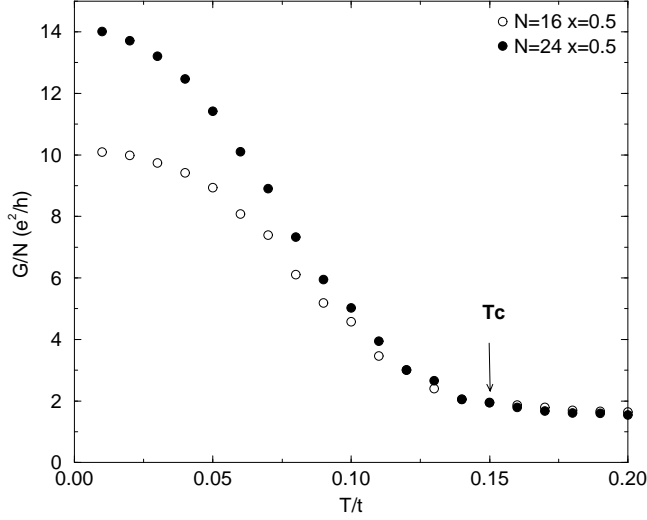


FIG. 3. Temperature dependence of the conductivity for the case of $x = 0.5$ and $N = 16$ and $N = 24$. The magnetic critical temperature T_c is pointed with an arrow. Above this temperature conductivity is independent of N .

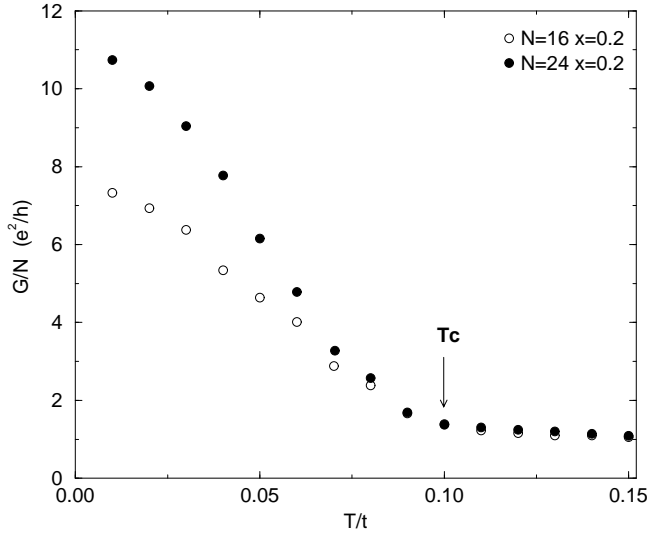


FIG. 4. Temperature dependence of the conductivity for the case of $x = 0.2$ and $N = 16$ and $N = 24$.

With respect to point a) we know that in the maximum disorder case ($T \rightarrow \infty$), the mobility edge is $|E_c| \sim 3.6t$. This energy is very close to the effective band edge and only less than 0.5% of the total states are localized. For lower temperatures we expect E_c to be closer to the effective band edge and the number of localized states should be even smaller. We are interested in values of $x > 0.1$ for which the chemical potential is much higher than E_c and for these electron concentrations we expect the system to be metallic at any T . The DE model is an insulator only at very small values of the electron concentration,

$x < 0.05$ and high temperatures. With respect to the elastic mean free path, point b), we find that the conductivity of the system decreases continuously with T , until it reaches the $T \rightarrow \infty$ limit (note that $G \sim \ell$). On the contrary if ℓ is bigger than the cluster size the transport is ballistic, the conductance is determined by the cluster size, and increases as N^2 . When ℓ is shorter than N the transport is diffusive and the conductance is proportional to N .

In Fig.3 we plot the conductance divided by N for $x=0.5$ and two values of the cluster size, $N=16$ and $N=24$. For low temperatures the core spins disorder is very weak and the elastic mean free path is larger than the cluster size. In this regime the transport is ballistic and the conductivity increases linearly with N . For large values of the temperature, G/N is independent of N . This is because the elastic mean free path is shorter than the cluster size and G/N is the electrical conductivity in units of the system lattice parameter. For $T > 0.12t$ the values of G/N obtained using $N = 16$ and $N = 24$ coincide, this implies that for these temperatures G/N is the conductivity. For $x = 0.5$ the magnetic critical temperature is $T_c \sim 0.15t$, and we can see in Fig.3 that the conductivity is a smooth function of T , practically constant, near T_c .

In Fig.4 we present the same quantity G/N as a function of T for $x = 0.2$. Also for this electron concentration the conductivity near T_c is a smooth function of T and the system is metallic. We have obtained similar results for different values of $x > 0.1$. The values for T_c are taken from reference [20].

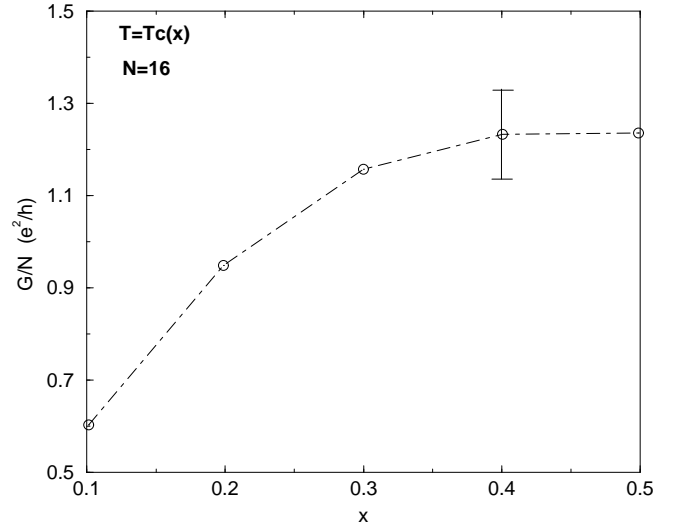


FIG. 5. Conductivity, evaluated at T_c , as a function of x . The dashed line is only a guide to the eye.

In Fig.5 we plot as a function of x , the value of the conductivity in lattice units evaluated at T_c . Using the value of 4\AA for the lattice parameter, we obtain a resistivity $\rho \sim 0.001\Omega - cm$ at $x = 0.2$ near T_c . This resistivity is around ten times smaller than the experimental ones, which also have an insulator-like dependence with T . This is a clear indication that it is necessary to add other terms to the double exchange Hamiltonian, in order to explain the occurrence of the metal insulator transition at temperatures near the magnetic critical temperature [24].

V. SUMMARY

We have calculated the temperature dependence of the electrical conductance of the double exchange Hamiltonian. The Kubo formula has been used for the calculation of the conductance. Conductance is defined as the average conductance over an statistical ensemble of clusters. These clusters are obtained by performing Monte Carlo simulations on the classical spin orientation of the double exchange Hamiltonian. The calculations have been done for different electron concentrations. We find that the system is metallic at all temperatures and, contrary to the mean field calculations, we do not observe any change in the temperature dependence of the resistivity near the magnetical critical temperature. Near T_c the resistivity we obtain is around ten times smaller than the experimental value. We conclude that the double exchange model is not able to explain the metal to insulator transition which experimentally occurs at temperatures near the magnetic critical temperature. Other effects not included in the DE Hamiltonian, as electron-electron interaction or electron-phonon interaction, are needed in order to understand the electrical behavior of the oxide Mn .

Acknowledgments. We thank Luis Martín-Moreno for useful discussions. This work was supported by the CI-CyT of Spain under Contract No. PB96-0085. MJC and LB also acknowledge financial support from the Fundación Ramón Areces.

[1] R.M. Kusters, J. Singleton, D.A. Keen, R. McGreevy and W. Hayes, *Physica (Amsterdam)* **155B**, 362 (1989); K. Chahara, T. Ohno, M. Kasai and Y. Kozono, *Appl. Phys. Lett.* **63**, 1990 (1993); R. von Helmolt, J. Wecker, B. Holzapfel, L. Schulzt and K. Samwer, *Phys. Rev. Lett.* **71**, 2331 (1993); S. Jin, T.H. Tiefel, M. McCormack, R.A. Fastnacht, R. Ramesh and J.H. Chen, *Science* **264**, 413 (1994).

[2] See, for example, A.P. Ramirez, *J. Phys.: Condens. Matter* **9**, 8171-8199 (1997); J.M.D. Coey, M. Viret and S. von Molnar, *Adv. in Phys.*, in press.

[3] N.F.Mott, in *Disorder Semiconductors* edited by M.A.Kastner, G.A.Thomas and S.R. Ovshinsky (Plenum, NY 1987).

[4] S. Yunoki and A. Moreo, *cond-mat/9712152*.

[5] E. Dagotto, S. Yunoki, A.L. Malvezzi, A. Moreo, J. Hu, S. Capponi, D. Poilblanc and N. Furukawa, *cond-mat/9709029*.

[6] D. Arovas and F. Guinea, *cond-mat/9711145*.

[7] S. Mori, C.H. Chen and S.-W. Cheong, *Nature*, **392**, 473 (1998); J.Millis *Nature*, **392**, 438 (1998).

[8] C. Zener, *Phys. Rev.* **82**, 403 (1951).

[9] P.W. Anderson and H. Hasegawa, *Phys. Rev.* **100**, 675 (1955).

[10] P.G. deGennes, *Phys. Rev.* **118**, 141 (1960).

[11] K. Kubo and N. Ohata, *J. Phys. Soc. Jpn.* **33**, 21 (1972).

[12] N.Furukawa, *J.Phys.Soc.Jpn.* **63**, 3214 (1994).

[13] A.J. Millis, B.I. Shraiman and R. Mueller, *Phys. Rev. Lett.* **77** 175 (1996).

[14] A.J. Millis, R. Mueller and B.I. Shraiman, *Phys. Rev. B* **54** 5405 (1996).

[15] E. Müller-Hartmann and E. Dagotto, *Phys. Rev. B* **54**, R6819 (1996).

[16] C.M.Varma, *Phys.Rev.B* **54**, 7328 (1996).

[17] Q. Li, J. Zang, A.R. Bishop and C.M. Soukoulis, *Phys. Rev. B*, **56**, 4541, (1997).

[18] R.Allub and B.Alascio, *Solid State Comm.* **99**, 613 (1996); and unpublished (*cond-mat/9608086*).

[19] J.M.Ziman, *J.Phys.C* **2**, 1230 (1969).

[20] M.J.Calderón and L.Brey, *Phys.Rev.B* in press.

[21] A. Bastin, C. Lewiner, O. Betbeder-Matibet, and P. Nozieres, *J. Phys. Chem. Solids* **32**, 1811 (1971).

[22] S. Datta, *Electronic Transport in Mesoscopic Systems* (Cambridge University Press, Cambridge, 1995).

[23] J.A. Vergés, *Phys. Rev. B* **57**, 870 (1998).

[24] A.J. Millis, P.B. Littlewood and B.I. Shraiman, *Phys. Rev. Lett.* **74**, 5144 (1995).